Bandwidth-controlled magnetic and electronic transitions in $La_{0.5}Ca_{0.5-x}Sr_xMnO_3$ ($0 \leqslant x \leqslant 0.5$) distorted perovskite

A. Sundaresan, P. L. Paulose, R. Mallik, and E. V. Sampathkumaran
Tata Institute of Fundamental Research, Homi Bhabha Road, Mumbai 400 005, India
(Received 14 October 1997)

We have investigated the effect of the increase of the one-electron e_g bandwidth (W) on the ferromagnetic and antiferromagnetic transitions in charge ordered $La_{0.5}Ca_{0.5}MnO_3$ by substituting bigger Sr^{2+} ions for Ca^{2+} ions through electrical resistivity and low-field ac-susceptibility measurements as a function of temperature. The system $La_{0.5}Ca_{0.5-x}Sr_xMnO_3$ is shown to undergo structural transitions with increasing x. For $x=0.0$ and 0.1, the structure is orthorhombic with space group $Pnma$. For $x=0.2$, 0.3, and 0.4, the structure is consistent with a monoclinic space group $I2/a$. The end member ($x=0.5$) has a tetragonal structure ($I4/mcm$). T_C increases with x monotonically, consistent with the fact that the increase of W enhances double-exchange ferromagnetic interaction. On the other hand, in contrast to the expected monotonic suppression, T_N increases initially with Sr concentration, followed by a decrease, finally disappearing for $x=0.4$. The nonmonotonous variation of T_N may indicate a possible change in the type of magnetic structure in the antiferromagnetic state. [S0163-1829(98)00306-3]

The distorted ABO_3-type perovskite $La_{0.5}Ca_{0.5}MnO_3$ is known to undergo transitions from a paramagnetic to a ferromagnetic state at $T_C \sim 225$ K and then to an antiferromagnetic state at $T_N \sim 150$ K.[1] In the paramagnetic state, the temperature dependence of electrical resistivity $\rho(T)$ is semiconductorlike and shows an anomaly at T_C, but does not show metallic behavior in the ferromagnetic region which is expected for double-exchange ferromagnetic interaction.[2] This is due to a smaller width (W) of the one-electron e_g band; W is determined by the average radius of the A-cations ($\langle r_A \rangle$) through Mn-O-Mn bond angles.[3] The low-temperature antiferromagnetic state, where $\rho(T)$ shows insulating behavior, has been attributed to simultaneous ordering of orbital (Jahn-Teller), charge (Mn^{3+} and Mn^{4+} ions) and spin (CE type).[4–6] The system $Nd_{0.5}Sr_{0.5}MnO_3$ with larger W ($\langle r_A \rangle = 1.2365$ Å) than that in $La_{0.5}Ca_{0.5}MnO_3$ ($\langle r_A \rangle = 1.198$ Å) shows a clear ferromagnetic metallic transition below $T_C (= 250$ K) and an antiferromagnetic nonmetallic transition setting in at $T_N = 160$ K as the temperature is lowered.[7] Recently, Kawano *et al.*[8] have reported that the system $Nd_{0.5}Sr_{0.5}MnO_3$ also exhibits an antiferromagnetic structure of the CE type whereas the material $Pr_{0.5}Sr_{0.5}MnO_3$ with a larger W ($\langle r_A \rangle = 1.2445$ Å) has an A-type spin arrangement, and they correlated this behavior with W. Further, they found no evidence for charge ordering in the antiferromagnetic state of $Pr_{0.5}Sr_{0.5}MnO_3$. On the other hand, the system $La_{0.5}Sr_{0.5}MnO_3$ with a still larger value of $\langle r_A \rangle$ ($=1.263$ Å) remains a ferromagnetic metal ($T_C = 230$ K) down to 2 K due to a larger W.[9]

The important effects of W on the ferromagnetic transition may be understood from the relationship $t_{ij} = b_{ij}\cos(\theta_{ij}/2)$; among the transfer integral (t_{ij}) of the e_g carriers between i and j Mn sites, the overlap integral (b_{ij}), and the relative angle (θ_{ij}) between the t_{2g} local spins.[10] Increase of W increases the overlap integral and hence the double-exchange interaction. At the same time, it modifies the charge-ordered antiferromagnetic structure and finally for larger W it destroys the antiferromagnetic state as mentioned earlier. Application of hydrostatical pressure also enhances the ferromagnetic interaction and modifies the antiferromagnetism in a similar way through an increase in the overlap integral.[11–13] In this article, we want to investigate whether the trends observed in the magnetic behavior as a function of W involving comparison of different systems (described in the previous paragraph) can be seen in a single system, viz., by the substitution of Sr for Ca in $La_{0.5}Ca_{0.5}MnO_3$.

Polycrystalline samples $La_{0.5}Ca_{0.5-x}Sr_xMnO_3$ ($x=0$, 0.1, 0.2, 0.3, 0.4, and 0.5) were prepared by the standard solid state method. Stoichiometric amounts of starting materials, La_2O_3 (Fluka AG; 99.98% dried at 1000 °C), $SrCO_3$, $CaCO_3$ (Leico Industries, New York; 99.999%), and MnO_2 (Cerac, 99.99%) were mixed thoroughly and calcined at 1100 °C. Then the products were pressed into pellets and sintered at 1500 °C for about 12 h, and cooled to room temperature at the rate of 5°/min. Powder x-ray diffraction data were collected using a JEOL diffractometer with CuK_α radiation by step scanning (0.02°) in the range $20° \leqslant 2\theta \leqslant 100°$. The data were analyzed by the Rietveld method using the program FULLPROF.[14] Ac susceptibility [$\chi(T)$] measurements (50–350 K) were performed with a frequency of 105 Hz and a driving field of 0.8 Oe. $\rho(T)$ measurements (4.2–300 K) were carried out by a four-probe method employing a conducting silver paste for making electrical contacts of the leads with the samples.

Powder x-ray diffraction patterns revealed that all the samples are single phase. X-ray data for $x=0$ and 0.1 could be refined on the basis of orthorhombic structure with the space group $Pnma$ as already reported for $La_{0.5}Ca_{0.5}MnO_3$,[15] and the pattern obtained at the convergence of the refinement is shown in Fig. 1. Occupancy of La

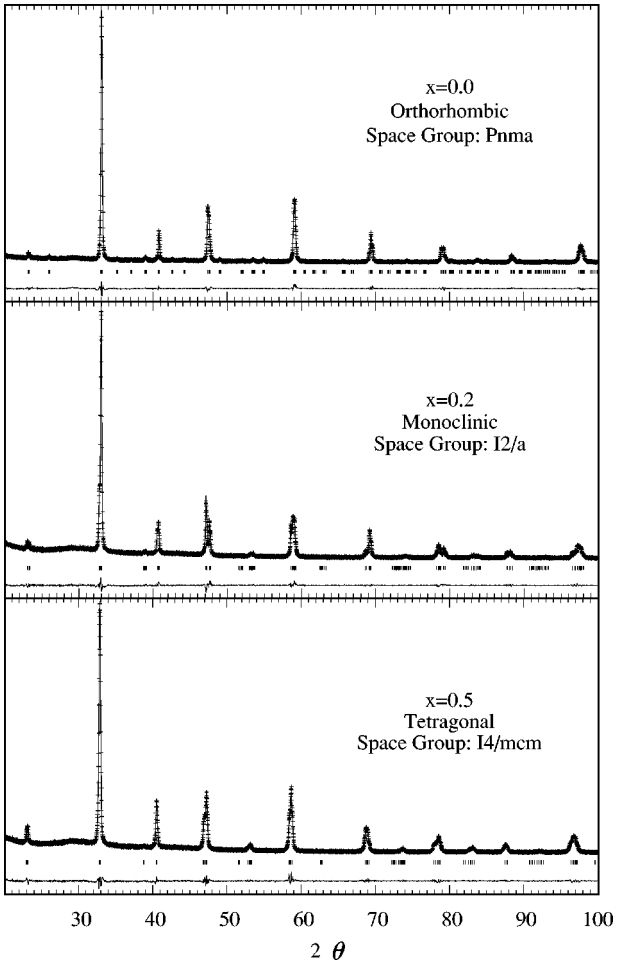

FIG. 1. Observed (pluses), calculated (continuous line), and difference patterns (at the bottom) of x-ray diffraction data for $x=0$, 0.2, and 0.5 fitted with orthorhombic ($Pnma$), monoclinic ($I2/a$), and tetragonal ($I4/mcm$), respectively, in $La_{0.5}Ca_{0.5-x}Sr_xMnO_3$. The vertical tick marks indicate the allowed reflections.

and Ca was refined with the constraint that the total occupancy was 1. This gives the ratio of La/Ca as 0.491(5)/0.509(5). Oxygen was assumed to be stoichiometric in all the samples. For $x=0.2$, the structure had changed and the extinction conditions limiting the hkl reflections are $h^2+k^2+l^2=2n$, consistent with an I-centered lattice. Furthermore, attempts to index the Bragg peaks on the orthorhombic and tetragonal lattices indicated that this phase had orthorhombic symmetry. Therefore, a refinement was carried out using the space group $Imma$ which is reported for $Nd_{0.5}Sr_{0.5}MnO_3$.[16] This refinement, however, did not give a satisfactory profile fit. A further refinement was made with a monoclinic lattice with the space group $I2/a$ which is found for $Pr_{0.6}Sr_{0.4}MnO_3$ at low temperatures.[17] This model gave the best fit to the observed data (see Fig. 1). The samples with $x=0.3$ and 0.4 are also found to form in the same structure. The single crystal sample with $x=0.47$ has been claimed by some to form in rhombohedral structure with the space group $R\bar{3}c$.[11] However, our attempt to refine the x-ray data of the polycrystalline sample based on this structure gave a poor fit and higher values of agreement factors. We find that this sample has a tetragonal symmetry with the space group $I4/mcm$ reported for $Pr_{0.5-x}Ce_xSr_{0.5}MnO_3$ with larger $\langle r_A\rangle$.[18,19] The observed, calculated, and difference patterns are also shown in Fig. 1. The refined structural parameters, bond lengths, and angles are given in Table I. It can be seen from the table that the cell volume increases with increase of x, consistent with the fact that the bigger Sr^{2+} ions are substituted at the Ca^{2+} site. Despite the lack of accuracy in the determination of oxygen positions with x-ray diffraction, the various bond lengths obtained are comparable to those found in similar systems.[18,19] In all these samples, only a small difference between the Mn-O(1) and Mn-O(2) bond distances is observed (<0.04 Å). This indicates that Jahn-Teller distortion is very small. Both the Mn-O(1)-Mn and Mn-O(2)-Mn bond angles increase with the increase of x as expected. In the case of $x=0.5$, the Mn-O(1)-Mn bond angle remains 180° because the octahedra are rotated about the longer c axis.

Results of ac $\chi(T)$ and $\rho(T)$ measurements while cooling and warming ($77\ \mathrm{K}\leqslant T\leqslant 300\ \mathrm{K}$) for the sample with $x=0$ are shown in Fig. 2(a). It can be seen from this figure that on cooling the ferromagnetic transition sets in at 220 K as reported earlier; the resistivity, however, shows a decrease with temperature below ~170 K and the decrease of susceptibility and increase of resistivity at about 130 K arise due to the onset of antiferromagnetic ordering. However, the resistivity values in the antiferromagnetic state remain low and the susceptibility does not seem to reach a nearly zero value at 77 K. It should be noted that this behavior is different from the one already reported[15] in the sense that the temperature derivative of $\rho(T)$ was found to be negative below T_N, with the corresponding value of the susceptibility being nearly zero. While warming, the antiferromagnetic state persists until about 175 K showing a large hysteresis, consistent with the first order nature of this transition. Corresponding hysteritic behavior is seen in ac χ data as well; there is a small hysteresis even at the ferromagnetic transition which is an artifact of the difficulties in controlling the rate of cooling. Similar results were also obtained for $x=0.05$ and are shown in Fig. 2(b). The discrepancies between the results reported in the literature and our findings are puzzling. It should be mentioned here that our results are reproducible under the present preparative conditions. Furthermore, the samples sintered at 1300 and 1400 °C also showed similar results. Therefore, it is possible that for our $x=0.0$ sample, oxygen is nonstoichiometric because of a low basicity of calcium (which is relieved, as we substitute higher basic Sr ions for Ca, *vide infra*). Another possibility is that the properties of this sample are sensitive to the quality of the starting materials because it is known that even 0.02 at. % of impurities can modify the metal-nonmetal transitions drastically in some manganites.[20] Further experiments such as neutron and electron diffraction are needed to have a complete characterization of this sample in order to understand the sample dependent properties.

Results of susceptibility and resistivity measurements for the other samples while warming are shown in Fig. 3. For $x=0.1$, the ac $\chi(T)$ (top panel) shows an antiferromagnetic to ferromagnetic transition at about 190 K and a ferromagnetic to paramagnetic transition at about 250 K. However, the $\rho(T)$ shows (bottom panel) a small change in slope at T_C but does not show a metallic behavior in the ferromagnetic

TABLE I. Structural parameters obtained from the Rietveld refinement of the room-temperature x-ray data for $x=0$, 0.2, and 0.5 in $La_{0.5}Ca_{0.5-x}Sr_xMnO_3$.

Parameters	$x=0$ ($Pnma$)	$x=0.2$ ($I2/a$)	$x=0.5$ ($I4/mcm$)
a(Å)	5.4179(2)	7.6392(4)	5.4444(2)
b(Å)	7.6390(3)	5.4689(3)	5.4444(2)
c(Å)	5.4283(3)	5.4350(3)	7.7527(4)
β(°)		89.98(1)	
V(Å^3)	224.66	227.06	229.8
(La,Ca,Sr)			
{x,y,z}	{0.0168(3), 1/4,−0.0020(9)}	{1/4, −0.002(1),0}	{0,1/2, 1/4}
B(Å^2)	0.425(4)	0.43(4)	0.21(4)
Mn{x,y,z}	{0,0,1/2}	{0,1/2,0}	{0,0,0}
B(Å^2)	0.425(4)	0.09(5)	0.06(4)
O(1)			
{x,y,z}	{0.496(2), 1/4,0.049(3)}	{1/4, 0.544(3),0}	{0,0,1/4}
B(Å^2)	0.8(1)	0.7(2)	1.3(1)
O(2)			
{x,y,z}	{0.274(3), 0.035(2), −0.280(3)}	{0.012(3), 0.231(4), 0.232(5)}	{0.239(4), 0.7239(4),0}
B(Å^2)	0.8(1)	0.7(2)	1.3(1)
χ^2	1.62	1.50	1.85
Bragg R(%)	4.11	3.95	3.09
Mn-O(1)×2 (Å)	1.928(2)	1.925(2)	1.938(1)
Mn-O(2)×2 (Å)	1.93(2)	1.94(2)	1.93(2)
Mn-O(2)×2 (Å)	1.97(2)	1.93(2)	1.93(2)
Mn-O(1)-Mn (°)	164.1(5)	166(2)	180.0(4)
Mn-O(2)-Mn (°)	159.9(7)	170(2)	175(1)

state expected for a double-exchange mediated ferromagnetism. The absence of metallic behavior may be due to smaller W because of smaller $\langle r_A \rangle$. Interestingly, just below T_N, the resistivity increases steeply and thus we are able to see the reported behavior for $x=0$. This implies that the substitution of more basic strontium makes the oxygen stoichiometric. Therefore, the magnetic structure in the antiferromagnetic state may be similar to that reported for $x=0$.[15] With a further increase of x, T_C increases monotonically. This is consistent with the fact that the increase of $\langle r_A \rangle$ increases the Mn-O-Mn bond angle (see Table I) and, therefore, W. The increase in W favors electron transfer and hence the ferromagnetic interaction. For $x=0.3$, a clear metallic behavior can be seen in the ferromagnetic region as expected for materials with larger W. On the other hand, T_N varies nonmonotonously with x; $T_N \sim 190$, 220, and 150 K for $x=0.1$, 0.2, and 0.3, respectively. Similar behavior has been observed in $Sm_{0.5-y}Pr_ySr_{0.5}MnO_3$,[21] $Nd_{0.5-z}La_zSr_{0.5}MnO_3$.[12] For $x=0.4$ and 0.5 the antiferromagnetic transition is destroyed and in these compositions, ferromagnetic metallic behavior is retained down to the lowest temperature measured. On the basis of the double-exchange interaction alone, one would expect that an increase of W should increase T_C and decrease T_N monotonously. The nonmonotonous variation of T_N with x from 0.0 to 0.3 presumably indicates the change in the magnetic structure (possibly from CE type to A type) as observed for $Nd_{0.5}Sr_{0.5}MnO_3$ and $Pr_{0.5-x}Ce_xSr_{0.5}MnO_3$.

In conclusion, this work brings out how a change in bandwidth caused by isoelectronic substitution at the Ca site in $La_{0.5}Ca_{0.5}MnO_3$ results in various structural, magnetic, and electrical behavior. For $x=0.0$, crystal structure (around 300 K) is orthorhombic with the space group $Pnma$ as already reported. For $x=0.2$, the structure is determined to be monoclinic ($I2/a$) and for the end member ($x=0.5$) the x-ray powder pattern could be best fit with a tetragonal structure with the space group $I4/mcm$. T_C increases monotonously with x, consistent with the fact that the double-

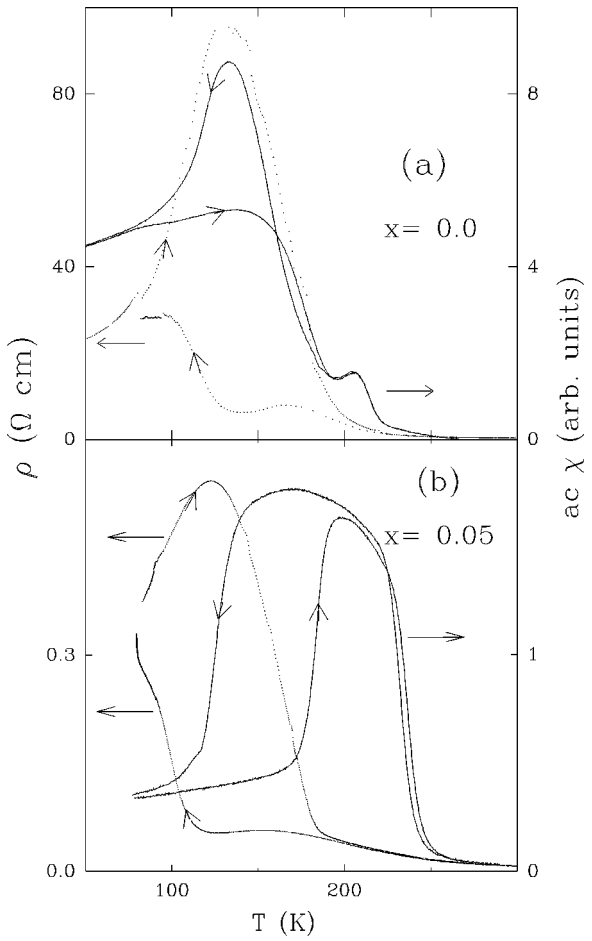

FIG. 2. (a) Resistivity (dots) and ac susceptibility (continuous line) measured as a function of temperature while cooling as well as warming for $La_{0.5}Ca_{0.5}MnO_3$. The resistivity data while cooling could be taken down to 77 K only, while the warming curve was obtained after cooling to 4.2 K. (b) Cooling and warming curves of resistivity and ac susceptibility for $La_{0.5}Ca_{0.45}Sr_{0.05}MnO_3$ above 77 K.

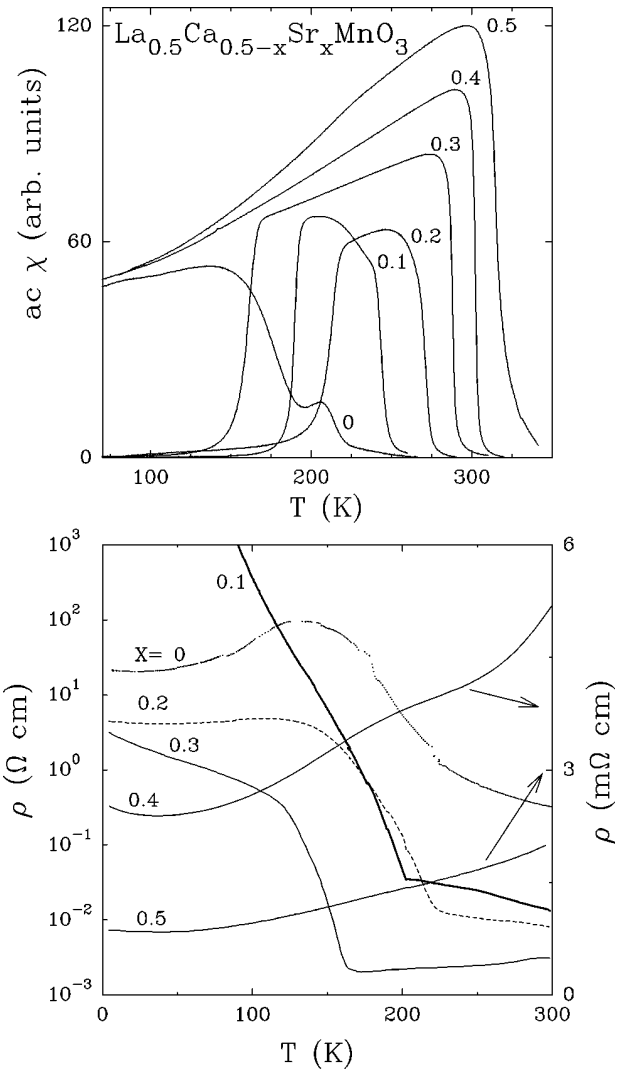

FIG. 3. ac susceptibility (top panel) and resistivity (bottom panel) versus temperature for $x=0.1$, 0.2, 0.3, 0.4, and 0.5 in $La_{0.5}Ca_{0.5-x}Sr_xMnO_3$ while warming.

exchange ferromagnetic interaction increases with W. On the other hand, T_N varies nonmonotonously with x, indicating a possible change in the type of magnetic structure in the antiferromagnetic state. Neutron measurements are essential for a deeper understanding of crystallographic and magnetic structures. In any case, it is clear from this work that this system will be useful in establishing the systematics in the bandwidth-controlled effects in manganites.

[1] P. Schiffer *et al.*, Phys. Rev. Lett. **75**, 3336 (1995).
[2] C. Zener, Phys. Rev. **82**, 403 (1951).
[3] N. Kumar and C. N. R. Rao, J. Solid State Chem. **129**, 363 (1997).
[4] J. B. Goodenough, Phys. Rev. **100**, 564 (1955).
[5] E. O. Wollan and W. C. Koehler, Phys. Rev. **100**, 545 (1955).
[6] P. G. Radaelli *et al.*, Phys. Rev. B **55**, 3015 (1997).
[7] H. Kuwahara *et al.*, Science **270**, 961 (1995).
[8] H. Kawano *et al.*, Phys. Rev. Lett. **78**, 4253 (1997).
[9] G. H. Jonker, Physica (Amsterdam) **XVI**, 337 (1950).
[10] P. W. Anderson and H. Hasegawa, Phys. Rev. **100**, 675 (1955).
[11] Y. Moritomo, A. Asamitsu, and Y. Tokura, Phys. Rev. B **51**, 16 491 (1995).
[12] Y. Moritomo *et al.*, Phys. Rev. B **55**, 7549 (1997).
[13] J. J. Neumeier, M. F. Hundley, J. D. Thompson, and R. H. Heffner, Phys. Rev. B **52**, R7006 (1995).
[14] J. Rodriguez-Carvajal (unpublished).
[15] P. G. Radaelli *et al.*, Phys. Rev. Lett. **75**, 4488 (1995).
[16] V. Caignaert *et al.*, Solid State Commun. **99**, 173 (1996).
[17] C. Ritter *et al.*, J. Solid State Chem. **127**, 276 (1996).
[18] D. N. Argyriou *et al.*, J. Solid State Chem. **124**, 381 (1996).
[19] A. Sundaresan *et al.* (unpublished).
[20] B. Raveau, A. Maignan, and C. Martin (private communication).
[21] F. Damay, A. Maignan, C. Martin, and B. Raveau, J. Appl. Phys. **81**, 1372 (1997).